Structure, stability and electronic properties of $SrSi_n$ ($n = 1$–12) clusters: Density-functional theory investigation*

Zhang Shuai(张 帅), Qin Yi(秦 怡), Ma Mao-Fen(马毛粉), Lu Cheng(卢 成)†, and Li Gen-Quan(李根全)

Physics & Electronic Engineering College, Nanyang Normal University, Nanyang 473061, *China*

(Received 17 April 2013; revised manuscript received 27 June 2013; published 6 December 2013)

Geometric structures, stabilities, and electronic properties of $SrSi_n$ ($n = 1$–12) clusters have been investigated using the density-functional theory within the generalized gradient approximation. The optimized geometries indicate that one Si atom capped on $SrSi_{n-1}$ structure and Sr atom capped Si_n structure for difference $SrSi_n$ clusters in size are two dominant growth patterns. The calculated average binding energy, fragmentation energy, second-order energy difference, the highest occupied molecular orbital, and the lowest unoccupied molecular orbital (HOMO–LUMO) gaps show that the doping of Sr atom can enhance the chemical activity of the silicon framework. The relative stability of $SrSi_9$ is the strongest among the $SrSi_n$ clusters. According to the mulliken population and natural population analysis, it is found that the charge in $SrSi_n$ clusters transfer from Sr atom to the Si_n host. In addition, the vertical ionization potential, vertical electron affinity, and chemical hardness are also discussed and compared.

Keywords: $SrSi_n$ clusters, ground state structure, stability, electronic properties

PACS: 36.40.−c, 36.40.Qv, 71.15.Mb **DOI:** 10.1088/1674-1056/23/1/013601

1. Introduction

Silicon is the most important semiconducting material in the microelectronics industry. Over the past decades, silicon clusters have attracted considerable attention both experimentally and theoretically,[1–8] because silicon possesses some unusual physical and chemical properties. Using the technique of laser vaporization supersonic expansion with metal carbonyl seeded carrier gas, Beck[9] studied the small mixed metal–silicon MSi_n (M = Cu, Cr, Mo, W) clusters by ArF and F_2 laser photoionization time-of-flight mass spectrometry. Nigam *et al.*[10] carried out a geometric and electronic structure calculation for Si_n, Si_n^+, and $AlSi_{n-1}$ ($n = 2$–13) clusters under linear combination of atomic orbital and molecular orbital (LCAO–MO) approach at the B3LYP/6-31G(d) level. Using first-principles density functional theory with generalized gradient approximation (DFT-GGA), Guo *et al.*[11] studied the geometries, stabilities, electronic and magnetic properties of the transition metal encapsulated MSi_n (M = Sc, Ti, V, Cr, Mn, Fe, Co, Ni, Cu, Zn; $n = 8$–16) clusters and found that every transition metal atom (TMA) fell into the center of Si outer frame and formed a metal-encapsulated Si cage at a certain size ($ScSi_{14}$, $TiSi_{12}$, VSi_{12}, $CrSi_{12}$, $MnSi_{11}$, $FeSi_{10}$, $CoSi_{10}$, $NiSi_{10}$, $CuSi_{12}$, and $ZnSi_{14}$). Chuang *et al.*[12] performed a low energy structure search for $AgSi_n$ clusters ($n = 1$–13) within the GGA to spin polarized DFT using projector-augmented-wave potentials. The calculated results indicated that Ag atom prefers to cap the Si clusters rather than be embedded inside Si clusters.

Strontium is an important alkali earth metal element. Although there are so many studies about metal atom doped MSi_n clusters, especially for 3d TM. To our best knowledge, no detailed theoretical investigation on the mixed strontium doped silicon clusters has been performed. There are still several essential open questions about the $SrSi_n$ clusters. What patterns of structure and chemical bonding exist in $SrSi_n$ clusters? Can Sr atoms in $SrSi_n$ clusters completely fall into the center of Si outer frame and form metal-encapsulated Si cage at a certain size? What are the charge properties of the $SrSi_n$ clusters? In order to clarify some of the above mentioned questions we study the equilibrium geometries, relative stabilities, and electronic properties of $SrSi_n$ ($n = 1$–12) clusters, and expect that such a theoretical study can provide helpful information for further theoretical and experimental studies about the metal atom doped MSi_n clusters.

2. Computational details

The geometrical optimizations of the $SrSi_n$ ($n = 1$–12) clusters are performed by using density functional theory with the unrestricted B3LYP exchange-correlation potential[13,14] of the generalized gradient approximation as implemented in the Gaussian 09 codes.[15] In the present calculations, full electron calculation for our studied system is rather time-consuming, so it is better to introduce the effective core potential LANL2DZ basis set[16] to describe the outermost valence electrons $3s^23p^2$ for Si atom and $4s^24p^65s^2$ for Sr atom. The convergence thresholds are set as 1.5×10^{-5} Hartree/Bohr for the forces, 6.0×10^{-5} Å for the displacement, and

*Project supported by the National Natural Science Foundation of China (Grant Nos. 11304167 and 51374132), the Postdoctoral Science Foundation of China (Grant No. 20110491317), the Natural Science Foundation of Henan Province, China (Grant Nos. 2011B140015 and 132300410290), and the Young Core Instructor Foundation of Henan Province, China (Grant No. 2012GGJS-152).

†Corresponding author. E-mail: lucheng@nynu.edu.cn

© 2014 Chinese Physical Society and IOP Publishing Ltd

10^{-6} Hartree for the energy change.[17] In searching for the ground-state structures, many possible initial isomers, which include one-, two-, and three-dimensional (3D) configurations, are considered staring from the previous optimized Si_n and XSi_n geometries. All clusters are relaxed fully without any symmetry constraints. Owing to the spin polarization, every initial configuration is optimized at possible spin multiplicities (singlet, triplet, and quintet).[18] All the ground-state structures are ensured that they have real vibrational frequency and a local minimum in potential energy.

To test the reliability and accuracy of our calculations, the Si_2, Sr_2, and SrSi dimers are studied. The bond lengths, vibrational frequency, vertical ionization potential, and fragmentation energy are listed in Table 1. For the Si_2 dimer, the calculated results are in good agreement with the experimental values and similar theoretical results.[19–23] For Sr_2 and SrSi dimers, there are no experimental and theoretical values available. Our calculated results are 5.45 Å, 23.07 cm^{-1}, 5.24 eV, and 0.04 eV for Sr_2, and 3.24 Å, 163.84 cm^{-1}, 6.10 eV, and 0.764 eV for SrSi, respectively. On the basis of the calculated results, it should be pointed out that the fragmentation energy of the SrSi dimer is greater than that of the Sr_2 dimmer, but smaller than that in the free Si_2 dimer. This reflects that in the $SrSi_n$ clusters the Si–Si interaction is stronger than the Sr–Si interaction and plays a dominant role in stabilizing the $SrSi_n$ clusters.

Table 1. Calculated values of bond length (r), vibrational frequency (ω), vertical ionization potential (VIP), and fragmentation energy (D) for Si_2, Sr_2, and SrSi molecules.

	Si_2			Sr_2			SrSi		
	Cal.	Theor.	Exp.	Cal.	Theor.	Exp.	Cal.	Theor.	Exp.
r/Å	2.35	2.29[a], 2.227[b], 2.279[c]	2.246[e]	5.45	–	–	3.24	–	–
ω/cm^{-1}	445.6	494[a], 568[b], 502[c]	511.0[e]	23.07	–	–	163.84	–	–
VIP/eV	8.81	–	8.15[e]	5.24	–	–	6.10	–	–
D/eV	2.62	2.62[d]	2.25[e]	0.04	–	–	0.76	–	–

[a] Ref. [19], [b] Ref. [20], [c] Ref. [21], [d] Ref. [22], [e] Ref. [23].

3. Results and discussion

3.1. Bare silicon cluster Si_{n+1}

In order to investigate the effect of dopant atom on the pure silicon clusters, we first optimize the pure Si_{n+1} (n = 1–12) clusters by using the identical method and basis set. The possible isomers of bare neutral silicon clusters for each cluster size have been extensively reported in previous literature,[24–26] and the lowest-energy geometric structures are only selected and shown in Fig. 1. We can see that the geometric structures and the symmetries are in line with the previous results. All the ground-state structures of Si_{n+1} clusters favor the 3D structures for n = 5–12 and planar structures for n = 1–4.

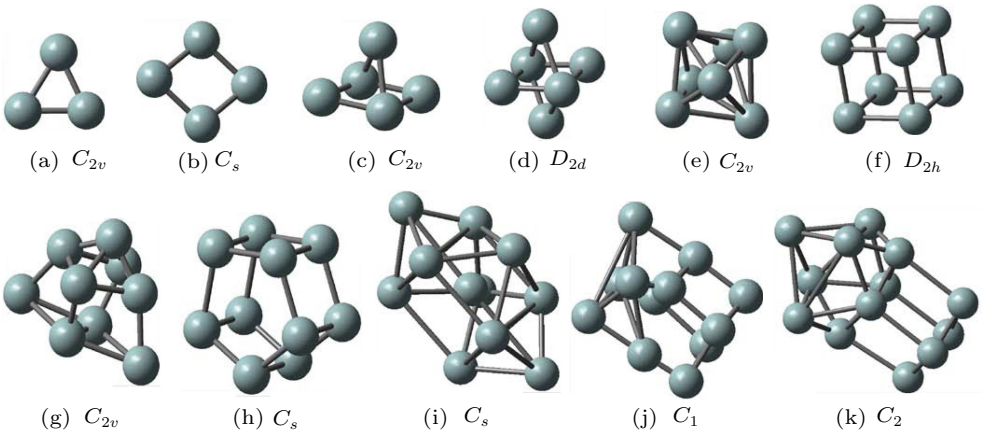


Fig. 1. (color online) The lowest-energy structures of (a) Si_3, (b) Si_4, (c) Si_5, (d) Si_6, (e) Si_7, (f) Si_8, (g) Si_9, (h) Si_{10}, (i) Si_{11}, (j) Si_{12}, and (k) Si_{13} clusters. The corresponding symmetries are presented by the B3LYP calculations.

3.2. Strontium-doped silicon cluster $SrSi_n$

Using the computational scheme described in Section 2, we have explored many low-lying isomers and determined the lowest-energy structures for $SrSi_n$ (n = 1–12) clusters. The obtained ground state and low-lying structures are displayed in Fig. 2. According to the relative energy from low to high, the stability orders of each cluster are designated by order of letter, na> nb> nc (n is the number of Si atoms in $SrSi_n$ clusters).

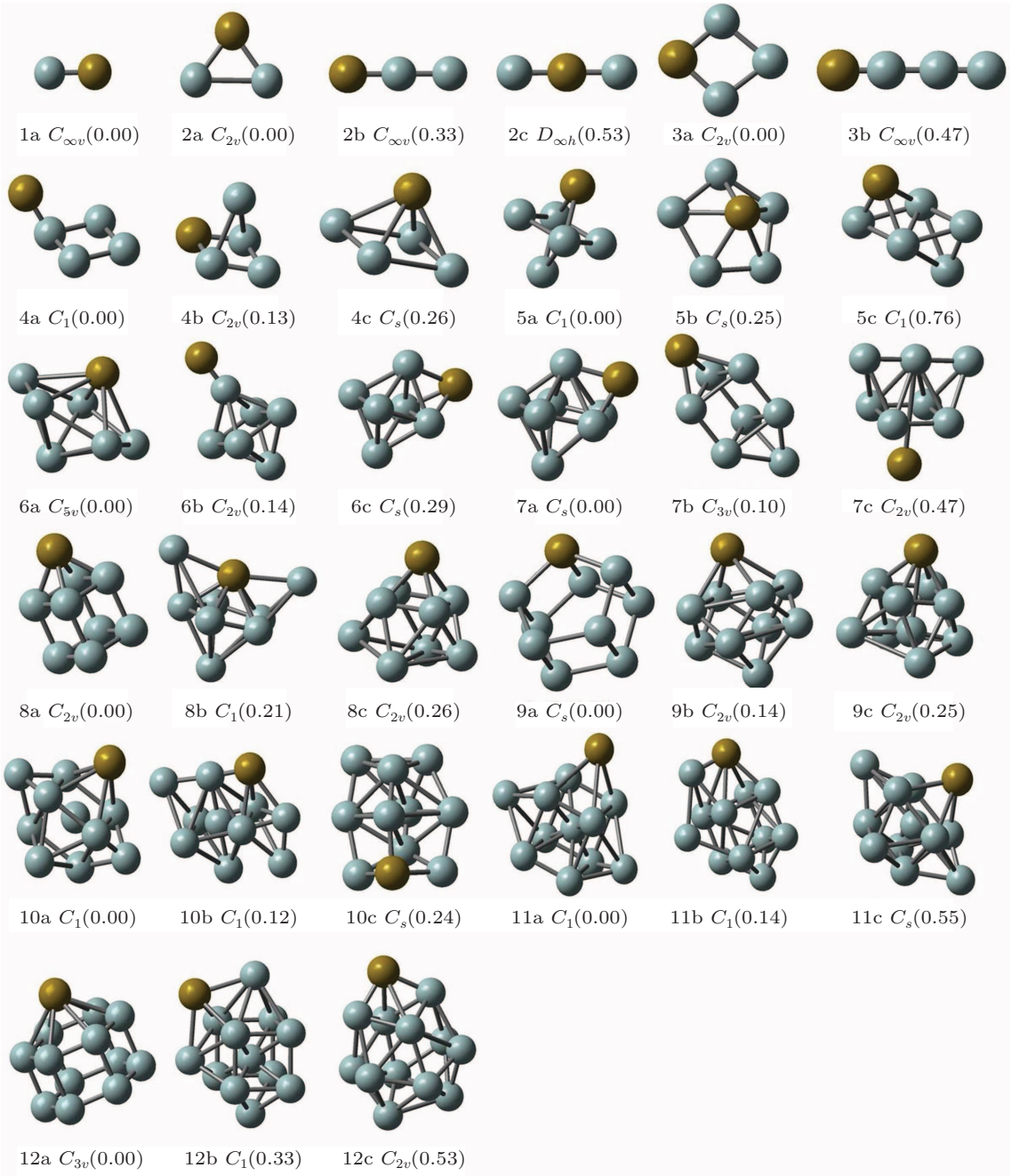


Fig. 2. (color online) The lowest-energy and low-lying structures of $SrSi_n$ ($n = 1$–12) clusters. The corresponding symmetries and energy difference compared to each of the ground state structures are presented by the B3LYP calculations.

The equilibrium geometry of the SrSi cluster with $C_{\infty v}$ symmetry is optimized. The triplet SrSi dimmer is the ground state, and the corresponding electronic state is $^3\sum$. The bond length of triplet SrSi dimer is 3.24 Å, which is longer than the Si–Si bond length, reflecting that the Sr–Si interaction is much weaker than the Si–Si interaction. The averaged bonding energy of SrSi dimer is 0.38 eV. For $SrSi_2$, the possible geometries such as C_{2v}, $C_{\infty v}$, and $D_{\infty h}$ isomers are optimized as the stable structures. According to the calculated results, it is worth noting that the lowest-energy structure shown in Fig. 2 (2a (C_{2v})) is an isosceles triangle in which the bond lengths are 3.20 Å for Sr–Si and 2.23 Å for Si–Si. For the bond angles, we obtained the values of 40.8° for Si–Sr–Si and 69.6° for Si–Si–Sr. The isomer 2a is similar to the lowest-energy structure of the Si_3 cluster. The linear structure 2b ($C_{\infty v}$) with Sr atom at one end is the next isomer with 0.33 eV higher in energy than the 2a isomer. Another linear structure 2c ($D_{\infty h}$) with Sr atom in the middle is the second metastable structure with 0.53 eV higher in energy than the 2a isomer. Among the isomers of $SrSi_3$, structure 3a has the lowest energy and real vibrational frequency, indicating it is the global minimum. Structure 3a is a planar rhombus with C_{2v} symmetry, which can be seen as Si trimer capped by one Sr atom or the Sr atom replacing one Si atom on the long diagonal of Si_4 (C_s) cluster. The linear structure 3b ($C_{\infty v}$) with Sr atom at one end is the next isomer with higher energy than the 3a isomer by 0.74 eV.

As the cluster size increases, the 3D structures prevail for $SrSi_n$ clusters at $n \geq 4$. We find that the most stable structure for $SrSi_4$ is one in which the edge of a C_s rhombus Si_4 is capped by one Sr atom, as shown in Fig. 2 (4a (C_1)). The metastable isomers of 4b (C_{2v}) and 4c (C_s) are both the pyramids, and their difference is the position of Sr atom. The energies of the isomer 4b and 4c are higher than that of the ground state structure 4a by 0.13 eV and 0.26 eV, respectively. With regard to the $SrSi_5$ cluster, three isomers are presented. The isomer 5a with C_1 symmetry, which can be obtained by substituting one Si atom at the top of tetragonal bipyramid Si_6, is the lowest-energy structure. Among $SrSi_5$ clusters, 5a has the largest VIP value 6.68 eV. The second isomer 5b is a pentagonal pyramid with Sr atom on the vertex. The isomer 5c can be viewed as capping two atoms on the ground state structure 3a. In the case of $SrSi_6$ cluster, the 6a isomer with C_{5v} symmetry is the most stable structure in all isomers. It can be viewed as attaching one Si atom on the most stable structure of $SrSi_5$ or substituting one Si atom at the top of pentagonal bipyramid Si_7. The isomer 6b with C_{2v} symmetry, which can be obtained by capping one Sr atom on the ground state structure 5a, is above the lowest-energy structure 6a by 0.14 eV. The 6c isomer with C_s symmetry is higher in energy than the 6a isomer by 0.29 eV. For $n = 7$, three isomers are plotted in Fig. 2 (7a–7c). The 7a isomer with C_s symmetry is found to be the most stable structure among all isomers. It can be seen that the ground-state structure of 7a is developed from the lowest energy structure of 6a by attaching one Si atom. The other isomers ((7b, C_{3v}), (7c, C_{2v})) have weaker stabilities than 7a as their energies are higher than that of the 7a isomer by 0.10 eV and 0.47 eV, respectively. As for the $SrSi_8$ cluster, three kinds of structures can be verified to be the minima. The isomer 8a with C_{2v} symmetry is evaluated to be the ground-state structure which can be regarded as capping one Si atom on the top of the hexahedral Si_8. The isomer 8b can be viewed as one Si atom capping on the ground-state $SrSi_7$ cluster. However, its energy is higher than that of the 8a isomer by 0.21 eV. The geometry of isomer 8c is similar to the structure of isomer 8a. However, the energy of 8c is higher than that of 8a by 0.26 eV. The low energy isomers for $SrSi_9$ are plotted in ((9a, C_s), (9b, C_{2v}), (9c, C_{2v})). The isomer 9a with C_s symmetry is found to be the most stable structure among all isomers, which is similar to the ground-state structure of pure Si_{10}. Among $SrSi_9$ clusters, isomer 9a has the largest second-order energy difference value. The theoretical value is 0.84 eV. Likewise, we identified three low energy isomers for $SrSi_{10}$, as shown in Fig. 2. The calculations show that the isomer 10a with C_1 symmetry is the ground-state structure. The isomer 10b with C_1 symmetry is the second stable structure, which is expected to be the lowest energy structure. However, its energy is higher by 0.12 eV than that of isomer 10a. The isomer 10c with C_s symmetry is above the isomer 10b by 0.12 eV. When the number of $SrSi_n$ cluster is up to 11, three stable isomers denoted as 11a (C_1), 11b (C_1), and 11c (C_s) are optimized to be the minima at the energy surface. The lowest-energy isomer shown in Fig. 2 (11a, C_1) is identified as one silicon atom capping on $SrSi_{10}$ in Fig. 2 (10a). Finally, three low energy isomers for $SrSi_{12}$ cluster are displayed in Fig. 2 ((12a, C_{3v}), (12b, C_1), (12c, C_{2v})). The calculation shows that the isomer 12a with C_{3v} symmetry is the ground-state structure.

From the above discussion, it is obvious that the most stable structures of $SrSi_n$ clusters favor the 3D structures for $n = 4$–12 and planar structures for $n = 1$, 2, 3. During the search for the lowest-energy structures of $SrSi_n$ clusters, the initial geometries with the Sr-encapsulated in the Si cage structures are also considered. The optimization results show that the Sr atom always prefers to cap on the outer frame. This property is quite different from some TM-doped Si clusters, such as $CrSi_n^-$ ($n = 3$–12), $CuSi_n^-$ ($n = 4$–18), $CoSi_n$ ($n = 1$–13), and $CuSi_n$ ($n = 9$–15),[27–30] but is quite similar to the $AgSi_n$ clusters.[12]

3.3. Relative stabilities

In this section, we have discussed relative stability of the most stable $SrSi_n$ ($n = 1$–12) clusters by the averaged binding energy $E_b(n)$, fragmentation energy $D(n)$, and the second-order energy difference $\Delta_2E(n)$. For the electronic properties, we calculate the HOMO–LUMO energy gaps E_{gap}, charge transfer, vertical ionization potential (VIP), and vertical electron affinity (VEA). The theoretical calculations are summarized in Table 2.

The $E_b(n)$, $D(n)$, and $\Delta_2E(n)$ for the $SrSi_n$ clusters can be expressed by

$$E_b(n) = [nE_k(Si) + E_k(Sr) - E_k(SrSi_n)]/(n+1), \quad (1)$$

$$D(n) = E_k(SrSi_{n-1}) + E_k(Si) - E_k(SrSi_n), \quad (2)$$

$$\Delta_2E(n) = E_k(SrSi_{n+1}) + E_k(SrSi_{n-1}) - 2E_k(SrSi_n), \quad (3)$$

where E_k is the total energy of the most stable Si atom, Sr atom, $SrSi_n$ clusters, $SrSi_{n-1}$ cluster, and $SrSi_{n+1}$ cluster, respectively.

Considering the influence of the impurity atom on small pure silicon clusters, all of the above calculations are compared with the pure Si_{n+1} clusters. The averaged binding energy $E_b(n)$, fragmentation energy $D(n)$, and the second-order energy difference $\Delta_2E(n)$ for the pure Si_{n+1} clusters are also studied using the following formulae:

$$E_b(n) = [(n+1)E_k(Si) - E_k(Si_{n+1})]/(n+1), \quad (4)$$

$$D(n) = E_k(Si_{n-1}) + E_k(Si) - E_k(Si_n), \quad (5)$$

$$\Delta_2E(n) = E_k(Si_{n+1}) + E_k(Si_{n-1}) - 2E_k(Si_n), \quad (6)$$

where E_k denotes the total energy of the most stable structures for Si, Si_{n+1}, Si_{n-1}, and Si_n clusters, respectively.

Table 2. Electronic state, symmetry, averaged binding energy (E_b), second-order energy difference ($\Delta_2 E$) , fragmentation energy (D) and the HOMO–LUMO energy gaps (E_{gap}) of the lowest energy structures for $SrSi_n$ ($n = 1$–12) clusters.

Cluster	State	Symmetry	E_b/eV	$\Delta_2 E$/eV	D/eV	E_{gap}/eV
SrSi	$C_{\infty v}$	$^3\Sigma$	0.38	–	0.76	2.36
$SrSi_2$	C_{2v}	$^1A_1$	1.29	−0.25	3.11	1.07
$SrSi_3$	C_{2v}	$^1A'$	1.81	0.82	3.36	1.77
$SrSi_4$	C_1	^1A	1.95	−0.77	2.54	1.29
$SrSi_5$	C_1	^1A	2.18	0.59	3.30	1.86
$SrSi_6$	C_{5v}	^1A	2.26	0.09	2.72	1.76
$SrSi_7$	C_s	^1A	2.30	−0.64	2.63	1.46
$SrSi_8$	C_{2v}	^1A	2.41	−0.15	3.27	1.24
$SrSi_9$	C_1	^1A	2.56	0.84	3.42	1.76
$SrSi_{10}$	C_1	^1A	2.52	−0.58	2.58	1.69
$SrSi_{11}$	C_1	^1A	2.57	0.02	3.15	1.53
$SrSi_{12}$	C_{3v}	^1A	2.61	–	3.13	1.68

Figure 3 presents the size dependence of the averaged binding energy E_b for the lowest-energy structures of $SrSi_n$ and pure Si_{n+1} clusters. As seen from Fig. 3, the curves of $E_b(n)$ for $SrSi_n$ and Si_{n+1} clusters show the same growing tendency as that of the cluster size. When $n \leq 5$, the $E_b(n)$ rapidly increase as the cluster size of the pure Si_{n+1} and $SrSi_n$ clusters increase, where the $E_b(n)$ of $SrSi_n$ clusters are much smaller than those of pure Si_{n+1} clusters. For $n > 5$, $E_b(n)$ of the pure Si_{n+1} and $SrSi_n$ clusters increases smoothly as the cluster size grows, and the $E_b(n)$ values of $SrSi_n$ clusters are still slightly smaller than that of pure Si_{n+1} clusters. Moreover, the $E_b(n)$ values of the $SrSi_n$ clusters are always smaller than that of pure Si_{n+1} clusters, which suggests that the Sr atom cannot enhance the stability of silicon clusters with small size. Both curves exhibit small peaks for Si_{n+1} ($n = 9$ and 12) and $SrSi_n$ ($n = 9$ and 12) clusters, indicating an enhanced stability over the adjacent neighboring clusters.

The second-order energy difference $\Delta_2 E(n)$ is a sensitive quantity that reflects the stability of clusters and it can be directly compared with the relative abundances determined in mass spectroscopy experiments.[31] The size dependence of $\Delta_2 E(n)$ for the lowest-energy pure Si_{n+1} and $SrSi_n$ clusters are shown in Fig. 4. It is clearly to note that the two curves for the Si_{n+1} and $SrSi_n$ clusters show irregular oscillating behavior and almost have the same tendency except $n = 11$. For the pure Si_{n+1} clusters, the local maxima correspond to cluster size with $n = 3$, 5, and 9. This implies that such clusters are relatively stable. It is in good agreement with the already established findings that clusters such as Si_4, Si_6, and Si_{10}, which have been identified as "magic numbers" for small Si_n clusters.[20,32] For the $SrSi_n$ clusters, maxima are found at cluster size with $n = 3$, 5, 9, and 11. The relative stability of $SrSi_9$ is the strongest among all the clusters based on the calculated second-order energy difference. Furthermore, Si_{10} and $SrSi_9$ clusters with the same geometrical structure have the largest $\Delta_2 E$ value, which is consistent with larger value shown in E_b plot at $n = 10$ (Fig. 3). This result can provide a satisfactory explanation of the fact that Si_{10} is a magic number cluster with high stability.

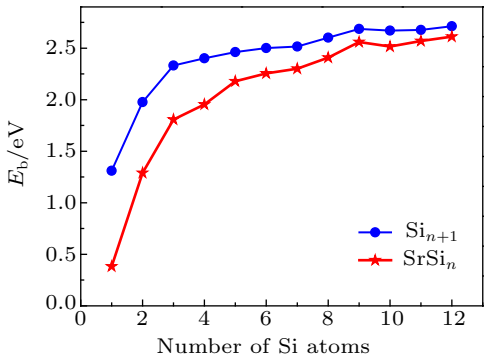


Fig. 3. (color online) Size dependence of the averaged binding energy $E_b(n)$ of the lowest energy structures for $SrSi_n$ and Si_{n+1} clusters.

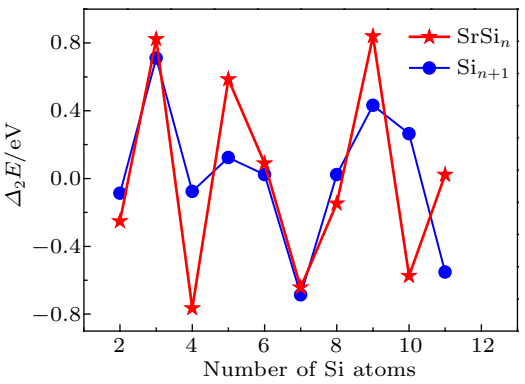


Fig. 4. (color online) Size dependence of the second-order energy difference $\Delta_2 E(n)$ for the lowest energy structures of $SrSi_n$ and Si_{n+1} clusters.

The fragmentation energy $D(n)$ is another sensitive quantity that reflects the relative stability of the surveyed clusters.[33,34] The $D(n)$ implicates the minimum energy of one Si atom when it is separated from the host clusters. The $D(n)$ of the lowest-energy structures for the pure Si_{n+1} and $SrSi_n$ clusters are calculated and shown in Fig. 5. It can be seen from Fig. 5 that the two curves have the similar tendency

except for $n = 11$ and 12. There are four remarkable peaks at cluster size with $n = 3$, 5, 9 and 12 for the pure Si_{n+1} clusters. These clusters have enhanced stability as compared to their neighbors, which agrees with photo-fragmentation spectra of mass-resolved Si_2–Si_{12}^+ clusters.[35–38] For the $SrSi_n$ clusters four prominent maxima $D(n)$ are found at $n = 3$, 5, 9, and 11. This result indicates that the ground-state structures of $SrSi_3$, $SrSi_5$, $SrSi_9$, and $SrSi_{11}$ cluster are more stable than its neighboring ones, which are well consistent with the maxima presented in the second-order energy difference $\Delta_2 E(n)$.

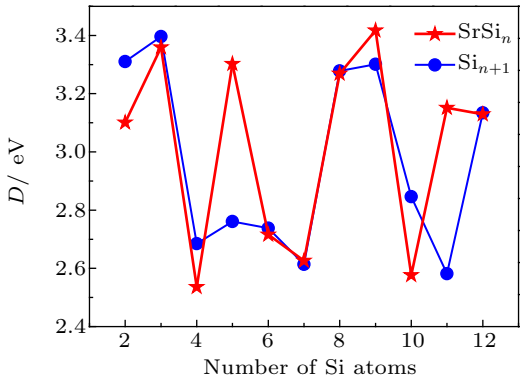


Fig. 5. (color online) Size dependence of the fragmentation energy $D(n)$ for the lowest-energy structures of $SrSi_n$ and Si_{n+1} clusters.

3.4. Electronic properties

The HOMO–LUMO energy gap E_{gap} reflects the ability for electrons to jump from occupied orbital to unoccupied orbital.[39,40] For the most stable structures of the pure Si_{n+1} and $SrSi_n$ clusters, the size dependence of the E_{gap} are plotted in Fig. 6. It can be seen from Fig. 6 that the two curves show the similar oscillation tendency except for $n = 1$ and 2. For the pure Si_{n+1} clusters, four remarkable peaks at $n = 3$, 5, 9, and 12, which implies that Si_4, Si_6, Si_{10}, and Si_{13} clusters, have larger E_{gap} than others. It means that Si_4, Si_6, Si_{10}, and Si_{13} clusters possess dramatically enhanced chemical stability. This is in agreement with $E_b(n)$, $\Delta_2 E(n)$, and $D(n)$ results shown in Figs. 3–5, respectively. For the $SrSi_n$ clusters, five prominent maxima are found at $n = 1$, 3, 5, 9, and 12. There are a maximum at $SrSi_1$ and a minimum at $SrSi_2$. The E_{gap} of $SrSi_2$ is 1.07 eV, which is the smallest one among the clusters. It is seen that the E_{gap} of $SrSi_n$ clusters are much smaller than those of the corresponding Si_{n+1} clusters as the cluster size increase when $n = 2$–12. This phenomenon indicates that the doped Sr atom can enhance the chemical activity of silicon clusters.

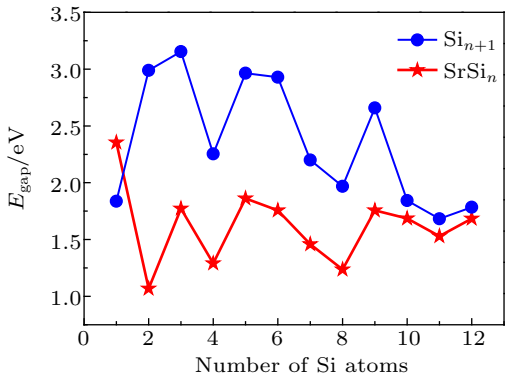


Fig. 6. (color online) Size dependence of the HOMO–LUMO energy gaps E_{gap} for the lowest-energy structures of $SrSi_n$ and Si_{n+1} clusters.

In order to investigate the reliable charge transfer information of $SrSi_n$ clusters, the Mulliken charge population (MP) and natural population (NP) for the lowest-energy $SrSi_n$ species have been calculated. The results are summarized in Table 3. It can be clearly seen that the values of MP and NP for the Sr atom in the $SrSi_n$ clusters possess positive 0.259–0.807 e and 0.494–1.350 e, respectively. This result indicates that the charges transfer from Sr atom to the Si_n frame, namely, Sr acts as electron donor in all $SrSi_n$ clusters.

Table 3. Mulliken charge population (MP) and natural population (NP) of Sr atom in the lowest-energy $SrSi_n$ ($n = 1$–12) clusters.

Cluster	SrSi	$SrSi_2$	$SrSi_3$	$SrSi_4$	$SrSi_5$	$SrSi_6$	$SrSi_7$	$SrSi_8$	$SrSi_9$	$SrSi_{10}$	$SrSi_{11}$	$SrSi_{12}$
MP	0.259	0.347	0.455	0.481	0.606	0.681	0.784	0.726	0.744	0.777	0.792	0.807
NP	0.494	0.878	0.846	0.644	1.063	1.049	1.175	1.350	1.207	1.225	1.246	1.296

The vertical ionization potential (VIP) and vertical electron affinities (VEA) are two significant parameters to gain a fundamental insight into the electronic properties.[41,42] The VIP and VEA are obtained by following formulas:

$$\mathrm{VIP} = E_{(\text{cation at optimized neutral geometry})} - E_{(\text{optimized neutral})}, \quad (7)$$

$$\mathrm{VEA} = E_{(\text{optimized neutral})} - E_{(\text{anion at optimized neutral geometry})}. \quad (8)$$

For the $SrSi_n$ clusters, no experimental data are available and the calculated VIP and *VEA* are given in Table 4. As shown in Table 4, VIP values of $SrSi_n$ clusters are markedly lower than those of Si_{n+1} clusters. The variation of the VIP with cluster size is mainly owing to the sum of valence electrons of all atoms. In other words, it is more difficult for Si_{n+1} clusters to lose electrons than $SrSi_n$ clusters. This suggests that the doped Sr atom can enhance the chemical activity of silicon clusters, which is in agreement with the previous analysis based on the $E_b(n)$. $SrSi_5$ has larger VIP value, corresponding to its higher stability. For $SrSi_n$ clusters, the values of VEA increase with increasing cluster size. The VEA value for the $SrSi_{12}$ cluster is the largest, implying that this cluster most easily acquires an electron.

Table 4. Vertical ionization potential (VIP) and vertical electron affinity (VEA) of the lowest energy structures for $SrSi_n$ and Si_{n+1} clusters.

Cluster	$SrSi_n$			Si_{n+1}			
	η	VIP/eV	VEA/eV	η	VIP/eV	VEA/eV	VIP/eV
SrSi	5.62	6.10	0.48	6.95	8.81	1.86	8.15 [a]
$SrSi_2$	4.12	5.98	1.86	7.19	8.81	1.62	8.0 ± 0.3 [b]
$SrSi_3$	4.75	6.43	1.69	6.117	8.30	2.18	8.12 [c]
$SrSi_4$	4.33	5.93	1.61	6.797	8.51	1.72	8.34 [c]
$SrSi_5$	4.56	6.68	2.11	6.38	8.23	1.85	8.00 [c]
$SrSi_6$	4.52	6.50	1.98	6.277	8.53	2.25	8.18 [c]
$SrSi_7$	4.08	6.39	2.31	5.328	8.06	2.73	7.34 [c]
$SrSi_8$	4.25	6.55	2.30	5.641	8.05	2.41	7.79 [c]
$SrSi_9$	4.31	6.67	2.35	4.916	7.69	2.77	8.10 [c]
$SrSi_{10}$	4.23	6.59	2.36	4.617	7.44	2.82	7.20 [c]
$SrSi_{11}$	3.98	6.47	2.49	4.379	7.41	3.03	7.03 [c]
$SrSi_{12}$	4.08	6.58	2.50	4.381	7.35	2.97	7.20 [c]

[a] Ref. [20], [b] Ref. [43], [c] Ref. [44].

3.5. Chemical hardness

Chemical hardness η has been used to characterize the relative stability of molecules and aggregate through the principle of maximum hardness (PMH) proposed by Pearson.[45,46] In terms of the finite-difference approximation and the famous Koopmans theorem,[47] the η can be obtained by using the VIP and VEA: η = VIP–VEA. As seen from Fig. 7 the curves of η for $SrSi_n$ and Si_{n+1} clusters show the same decreasing tendency with increasing cluster size. The local maxima occur at Si_3, Si_5, Si_9, SrSi, $SrSi_3$, $SrSi_5$, and $SrSi_9$, which reflects that these structures are harder than their neighboring clusters. The SrSi cluster shows the largest η (562 eV), which indicates that the cluster is extremely inert and should be useful to fabricate the cluster-assembled nanomaterials.[19] Furthermore, for the pure silicon clusters, it keeps a high hardness in comparison with the $SrSi_n$ clusters with the increasing cluster size. This shows that the doped Sr atom can reduce the chemical hardness of Si_{n+1} cluster.

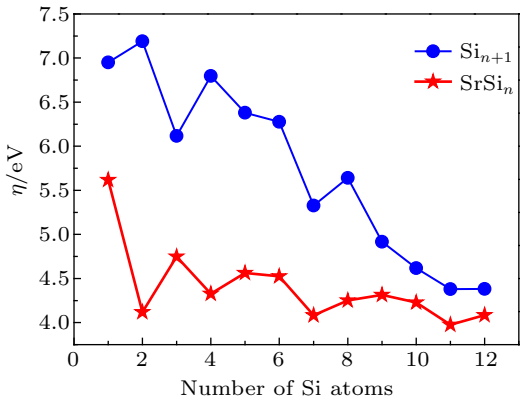


Fig. 7. (color online) Size dependence of the chemical hardness η for the lowest-energy structures of $SrSi_n$ and Si_{n+1} clusters.

4. Conclusion

The geometrical structures, stabilities, and electronic properties of the $SrSi_n$ (n = 1–12) clusters have been systematically investigated by the first-principles calculations. The optimized geometries show that one Si atom capped on $SrSi_{n-1}$ structure and Sr atom capped Si_n structures for different sized $SrSi_n$ (n = 1–12) clusters are two dominant growth patterns. The lowest-energy structures of $SrSi_n$ clusters favor the planar structures for n = 1–3 and 3D structures for n = 4–12. According to the calculated results of $E_b(n)$, $D(n)$, $\Delta_2 E(n)$, and E_{gap}, the dopant Sr atom in the $SrSi_n$ clusters enhance the chemical activity of the Si framework. The relative stability of $SrSi_9$ is the strongest among the investigated clusters. On the basis of the calculated Mulliken populations and natural populations, it is found that the charges in corresponding $SrSi_n$ clusters transfer from Sr atom to the Si_n frame.

References

[1] Raghavachari K and Rohlfing C M 1988 *Chem. Phys. Lett.* **143** 428
[2] Rohlfing C M and Raghavachari K 1990 *Chem. Phys. Lett.* **167** 559
[3] Chesnovsky O, Yang S H, Pettiette C L, Craycraft M J, Liu Y and Smlley R E 1987 *Chem. Phys. Lett.* **138** 119
[4] Nakajima A, Taguwa T, Nakao K, Gomei M, Kishi R, Iwata S and Kaya K 1995 *J. Chem. Phys.* **103** 2050
[5] Kishi R, Kawamata H, Negishi Y, Iwata S, Nakajima A and Kaya K 1997 *J. Chem. Phys.* **107** 10029
[6] Ho K M, Shvartsburg A A, Pan B, Lu Z Y, Wang C Z, Wacker J G, Fye J and Jarrold M F 1998 *Nature* **392** 582
[7] Hagelberg F, Leszczynski J and Murashov V 1998 *J. Mol. Struct: Theochem.* **454** 209
[8] Rata I, Shvartsburg A A, Horoi M, Frauenheim T, Michael K W and Jackson K A 2000 *Phys. Rev. Lett.* **85** 546
[9] Beck S M 1989 *J. Chem. Phys.* **90** 6306
[10] Nigam S, Majumder C and Kulshreshtha S K 2004 *J. Chem. Phys.* **121** 7756
[11] Guo L J, Zhao G F, Gu Y Z, Liu X and Zeng Z 2008 *Phys. Rev. B* **77** 195417
[12] Chuang F C, Hsieh Y Y, Hsu C C and Albao M A 2007 *J. Chem. Phys.* **127** 144313
[13] Becke A D 1988 *Phys. Rev. A* **38** 3098
[14] Lee C, Yang W and Parr R G 1988 *Phys. Rev. B* **37** 785
[15] Frisch M J, Clemente F R, Trucks G W and Trucks G W 2009 *Gaussian* 09 (Rev C.01) (Pittsburgh, PA: Gaussian Inc.)
[16] Hay P J and Wadt W R 1985 *J. Chem. Phys.* **82** 270
[17] Die D, Kuang X Y, Zhu B and Guo J J 2011 *Physica B* **406** 3160
[18] Li Y F, Kuang X Y, Wang S J, Li Y and Zhao Y R 2011 *Phys. Lett. A* **375** 1877
[19] Bruna P J, Peyerimhoff S D and Buenker R J 1980 *J. Chem. Phys.* **72** 5437

[20] Raghavachari K 1986 *J. Chem. Phys.* **84** 5672
[21] Nimlos M R, Harding B L and Ellison G B 1987 *J. Chem. Phys.* **87** 5116
[22] Han J G, Zhao R N and Duan Y H 2007 *J. Phys. Chem. A* **111** 2148
[23] Huber K P and Herzberg G 1979 *Molecular Spectra and Molecular Structure IV*, *Constants of Diatomic Molecules* (New York: van Nostrand/Reinhold) pp. 171–172
[24] Pouchan C and Bégue D 2004 *J. Chem. Phys.* **121** 4628
[25] Yang J C, Xu W G and Xiao W S 2005 *J. Mol. Struct: Theochem.* **719** 89
[26] Qin W, Lu W C, Zhao L Z, Zang Q J, Wang C Z and Ho K M 2009 *J. Phys.: Condens. Matter* **21** 455501
[27] Kong X Y, Xu H G and Zheng W J 2012 *J. Chem. Phys.* **137** 064307
[28] Xu H G, Wu M M, Zhang Z G, Yuan J Y, Sun Q and Zheng W J 2012 *J. Chem. Phys.* **136** 104308
[29] Ma L, Zhao J J, Wang J G, Lu Q L, Zhu L Z and Wang G H 2005 *Chem. Phys. Lett.* **411** 279
[30] Hossain D, Pittman Jr C U and Gwaltney S R 2008 *Chem. Phys. Lett.* **451** 93
[31] Sun H R, Kuang X Y, Li Y F, Shao P and Zhao Y R 2012 *Chin. Phys. B* **21** 083601
[32] Raghavachari K and Rohlfing C M 1988 *J. Chem. Phys.* **89** 2219
[33] Chen D D, Kuang X Y, Zhao Y R, Shao P and Li Y F 2011 *Chin. Phys. B* **20** 063601
[34] Li Y F, Mao A J, Li Y and Kuang X Y 2012 *J. Mol. Model.* **18** 3061
[35] Liu B, Lu Z Y, Pan B, Wang C Z, Ho K M, Shvartsburg A A and Jarrold M F 1998 *J. Chem. Phys.* **109** 9401
[36] Lu Z Y, Wang C Z and Ho K M 2000 *Phys. Rev. B* **61** 2329
[37] Shvartsburg A A, Liu B, Lu Z Y, Wang C Z, Jarrold M F and Ho K M 1999 *Phys. Rev. Lett.* **83** 2167
[38] Bloomfield L A, Freeman R R and Brown W L 1985 *Phys. Rev. Lett.* **54** 2246
[39] Li J, Liu X Y, Zhu Z H and Sheng Y 2012 *Chin. Phys. B* **21** 033101
[40] Shao P, Kuang X Y, Ding L P, Zhong M M and Wang Z H 2012 *Physica B* **407** 4379
[41] Liu Z F, Lei X L, Liu L R, Liu H Y and Zhu H J 2011 *Chin. Phys. B* **20** 023101
[42] Wang H Q, Kuang X Y and Li H F 2010 *Phys. Chem. Chem. Phys.* **12** 5156
[43] Drowart J, DeMaria G and Inghram M G 1958 *J. Chem. Phys.* **29** 1015
[44] Ma L, Zhao J J, Wang J G, Lu Q L, Zhu L Z and Wang G H 2005 *Chem. Phys. Lett.* **411** 279
[45] Pearson R G 1997 *Chemical Hardness: Applications from Molecules to Solids* (Weinheim: Wiley-VCH) pp. 76–78
[46] Ding L P, Kuang X Y, Shao P, Zhao Y R and Li Y F 2012 *Chin. Phys. B* **21** 043601
[47] Parr R G and Yang W 1989 *Density Functional Theory of Atoms and Molecules* (New York: Oxford University Press) pp. 125–128